RESEARCH ARTICLE doi.org/10.1002/adsc.202500066

ADVANCED SYNTHESIS & CATALYSIS

Multiphoton Multicomponent Reactions: Discovery of the 2-Photon Ketene 4-Component Reaction (2P-K-4CR)

Federica Minuto,[a] Martina Buccioli,[a] Pietro Capurro,[a] Barbara Benedetti,[a] Pavlo Solokha,[a] Serena De Negri,[a] Davide Ravelli,[b] and Andrea Basso[a,*]

[a] Department of Chemistry and Industrial Chemistry, University of Genova, Via Dodecaneso, I-16146 Genova, Italy
E-mail: andrea.basso@unige.it
[b] Department of Chemistry, PhotoGreen Lab, University of Pavia, Via Taramelli, I-27100 Pavia, Italy

Manuscript received: January 20, 2025; Revised manuscript received: May 6, 2025;
Version of record online: June 16, 2025

Supporting information for this article is available on the WWW under https://doi.org/10.1002/adsc.202500066

Abstract: Herein, the first multiphoton, multicomponent approach for synthesizing highly functionalized oxetanes using diazoketones, isocyanides, silanols (or carboxylic acids), and 1,2-dicarbonyl derivatives (benzils) is presented as starting materials. Blue light irradiation initiates the Wolff rearrangement of diazoketones, generating ketenes that promptly react with isocyanides and silanols (or carboxylic acids) to afford captodative olefins. Concurrently, excitation of benzils promotes a [2 + 2] photocycloaddition between the activated carbonyl group and the captodative olefin. This newly developed two-photon ketene four-component reaction has been thoroughly investigated, also through chemometric analysis, including its substrates scope and the extension to mixed benzils. Furthermore, the observed stereochemical outcomes, validated by X-Ray diffraction analysis, are elucidated through detailed computational studies, providing insights into the underlying reaction mechanism.

Keywords: multicomponent reactions, visible lights, oxetanes, Paternò–Büchi, diazoketones

1. Introduction

The oxetane ring is one of the most sought-after scaffolds in organic chemistry, owing to its broad synthetic and functional versatility. Over the years, various strategies have been explored for its construction, ranging from classical textbook methods to advanced engineered systems.[1–3] Key synthetic approaches include 1) ring opening and expansion of epoxides,[4,5] 2) ring contraction,[6] and 3) the Paternò–Büchi photochemical [2 + 2] cycloaddition.[7] The latter strategy typically involves the reaction of carbonyl compounds with alkenes, utilizing direct UV light irradiation, or the adoption of visible light in the presence of a competent photocatalyst.[8,9] More recently, the use of blue light has emerged as a valuable approach, exploiting the reactivity of aromatic 1,2-diketones (benzils); however, this approach has so far been limited to the synthesis of relatively simple structures.[10–12]

The integration of multicomponent reactions (MCRs) with photochemical transformations has garnered significant attention over the past decade, as evidenced by the increasing number of research articles and reviews on the topic.[13,14] This approach owes its success to the synergistic benefits of both methodologies, including high atom and step economy, excellent selectivity, mild reaction conditions, and the ability to generate structurally complex products. These attributes collectively position photoinduced MCRs (PMCRs) as an enabling approach toward greener and more sustainable chemical processes.

Although photochemistry can be conveniently exploited to elaborate previously assembled multicomponent adducts, most strategies based on PMCRs involve the activation of a single substrate—either

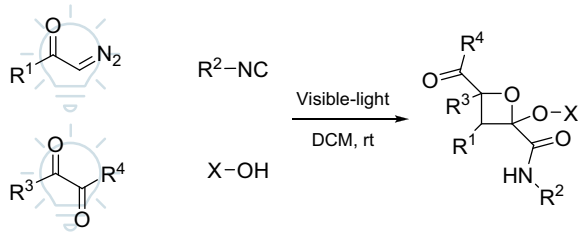

Scheme 1. General scheme of the 2P-K-4CR, characterized by a double photochemical activation, on the route to highly functionalized oxetane scaffolds.

directly or via a photoredox catalyst—to initiate the reactivity manifold of interest and the ensuing combination with the other components in the reaction. However, to the best of our knowledge, existing methods have exclusively relied on the interaction of light with a single substrate or catalyst, and there are no reported examples of multiphoton MCRs where radiation simultaneously activates two or more substrates.

The direct interaction of light with organic molecules can facilitate various processes, such as rearrangements (e.g., the Wolff rearrangement of diazoketones) or cycloadditions (e.g., carbonyl derivatives engaging olefins to form cyclic structures upon excitation). Recently, we reported the innovative combination of these processes in a single synthetic sequence. Specifically, we demonstrated that the irradiation of diazoketones and benzils with blue light yields oxetanones through a [2 + 2] Paternò–Büchi process. In this transformation, visible light induces the Wolff rearrangement of diazoketones to ketenes, while simultaneously activating benzils, therefore enabling the photocycloaddition as well.[15]

In the past, our group has extensively studied the use of ketenes in MCRs, leading to the development of α-acyloxy or α-silyloxy acrylamide scaffolds via the ketene three-component reaction (K-3CR)[16,17] and its silylative variant (SK-3CR).[18] These processes, involving ketenes, acidic species, and isocyanides, efficiently produce captodative olefins with complete *Z* selectivity under visible-light irradiation.[19] These compounds were successfully tested in various reactions, including a Paternò–Büchi photocycloaddition with a simple carbonyl compound under UV irradiation, yielding modest results.[18]

Motivated by these findings, we were intrigued to discover whether, in the presence of additional carbonyl derivatives such as benzils, the photogenerated ketene would prefer to undergo the [2 + 2] photocycloaddition pathway or the thermal multicomponent route previously reported. In this communication, we describe the discovery of a new MCR, namely the 2-photon ketene 4-component reaction (2P-K-4CR), that leads to the synthesis of highly functionalized oxetanes through a double photoactivation, with the incorporation of all four reagents in the final products (**Scheme 1**). A thorough study on the mechanism, selectivity aspects, and versatility of this reaction has been carried out, corroborated by the results of a computational analysis.

2. Results and Discussion

2.1. Experimental Results

In our initial experiment, we irradiated a mixture of phenyl diazoketone **1a**, triphenyl silanol **2a**, cyclohexyl isocyanide **3a**, and benzil **4a** with blue light. To our delight, neither oxetanone **D** (resulting from ketene/benzil photocycloaddition), nor captodative olefin **B** were detected. Instead, compound **5a**, incorporating all four reaction components, was generated in one step with the formation of four new bonds and three stereogenic carbons (**Scheme 2**). Remarkably, among all the possible isomers, only two new products, tagged as $\mathbf{5a_M}$ and $\mathbf{5a_m}$, were obtained. These products were isolated in a combined yield of 70%, with a $\mathbf{5a_M}$:$\mathbf{5a_m}$ ratio of 2.5:1, as determined by ^{1}H-NMR analysis. Careful NMR analysis of the purified products also revealed that $\mathbf{5a_M}$ and $\mathbf{5a_m}$ are diastereoisomers, both resulting from a regioselective cycloaddition of benzil **4a** to captodative olefin **B**. The evidence that the ketene deriving from **1a** prefers to react with **2a** and **3a**, rather than with excited **4a**, as well as the

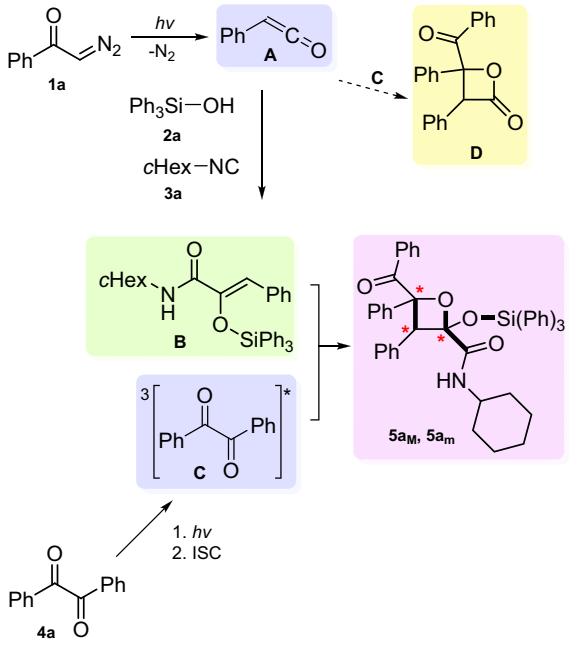

Scheme 2. 2P-K-4CR to oxetanes **5a**, characterized by a double photochemical activation. Irradiation of diazoketone **1a** results in the generation of ketene **A**, that in the presence of silanol **2a** and isocyanide **3a** affords olefin **B**. Upon irradiation, benzil **4a** is excited to triplet species **C**. The latter could react with **A**, affording oxetanone **D**, or with **B**, resulting in the formation of the isolated product **5a**.

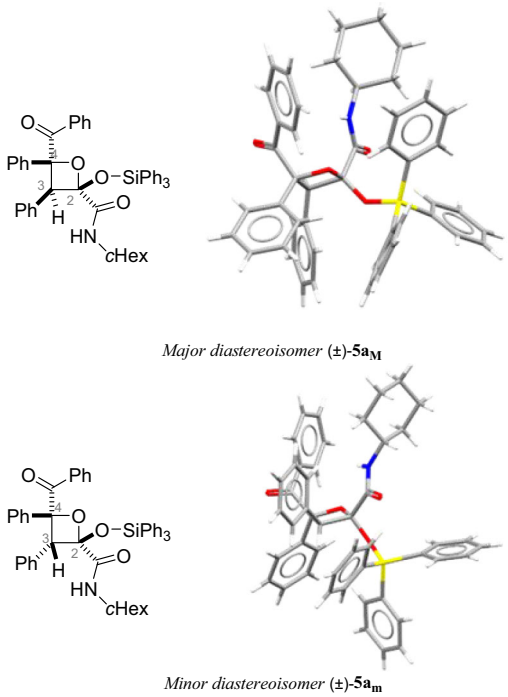

Figure 1. Molecular structure from XRD studies and representation of diastereoisomers **5a$_M$** and **5a$_m$**.

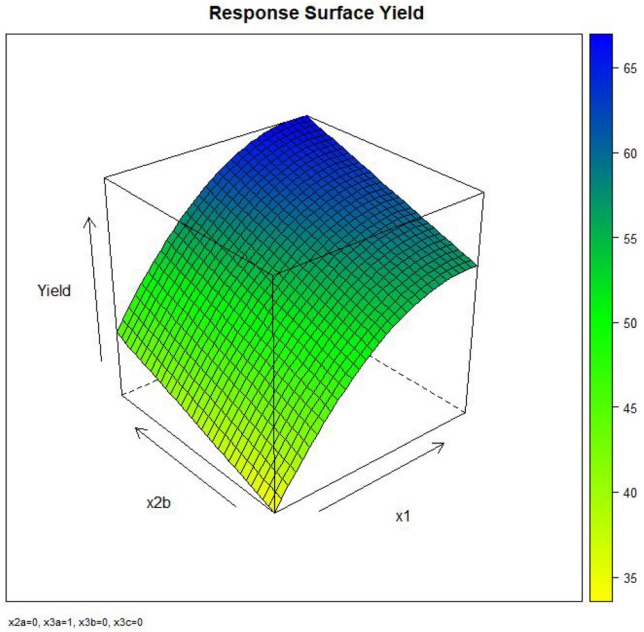

Figure 2. Response surface yield for DCM, where x1 is temperature and x2b is 450 nm.

selectivity of the cycloaddition between **B** and **4a**, is discussed in detail in the computational study section.

To univocally determine the relative configurations of diastereoisomers **5a$_M$** and **5a$_m$**, single-crystal X-Ray diffraction (XRD) analysis[20] was carried out (**Figure 1**). Interestingly, the relative stereochemistry at C-2 and C-4 was preserved, while the two diastereoisomers differed for the configuration at C-3.

Intrigued by the discovery of this new reaction, we next carried out an optimization of the reaction conditions adopting the design of experiment (DoE) approach, realizing a D-optimal design with the variables reported in **Table 1** (see Supporting Information for further information).[21–23] Performing a low number of experiments, dichloromethane (DCM) and 25 °C were identified as the best solvent and temperature, respectively, while both 450 and 470 nm irradiation wavelengths led to the same result in terms of yield (70%). The response surface yield for dichloromethane is reported in **Figure 2**.

Gratified by these results, a small library of compounds was prepared, assessing the versatility of the hereby disclosed 2P-K-4CR (**Table 2**). Aromatic and heteroaromatic diazoketones behaved as good partners in this MCR, with products **5a-c,i** formed selectively, although in low yield in the case of the thienyl derivative. Aliphatic (benzyl- and hexyl-) diazoketones failed to afford the desired products, in agreement with our previous report.[15] In addition to triphenyl silanol, *tert*-butyldiphenylsilanol also afforded product **5d**, demonstrating the possibility to introduce an alternative silyl group in these complex architectures. Thanks to similar reactivity, both silanols and carboxylic acids can be efficiently employed in the transformation. Thus, a satisfying performance was observed in the presence of acetic acid and 3,3-dimethylbutyric acid, which led to the isolation of products **5e** and **5f** with high yield. However, when benzoic acid was tested, unreacted benzil and captodative olefin[17] were isolated.

The K-3CR and SK-3CR can be efficiently carried out using various linear and cyclic isocyanides.[13] Also in the case of the hereby reported 2P-K-4CR, compound **5g** could be isolated from *n*-butyl isocyanide without any significant loss in reactivity.

Concerning carbonyl derivatives, 4-Br- and 4-Me-substituted benzils were tested and led to the isolation of the corresponding products **5h–j** in high yields. Compound **5h** was also prepared on a 1 mmol scale, affording comparable results. As previously reported,[10]

Table 1. Variables and levels of the D-optimal design realized for the optimization of the reaction conditions.

Variable ID	Variable	Levels			
X_1	Temperature (°C)	−15	5	25	–
X_2	Wavelength (nm)	405	450	470	–
X_3	Solvent	DCM	MeCN	tetrahydrofuran (THF)	Hexane

Table 2. Substrate scope of the two photon ketene four-component reaction (2P-K-4CR) (see Scheme 1). Conditions: DCM, 450 nm, at room temperature. For a figure displaying the structures of all synthesized products, see Section S4, Supporting Information.

Entry	R^1	R^2	X	$R^3 = R^4$	Yield[a)]	diastereomeric ratio
5a	Ph	*c*Hex	Ph_3Si	Ph	70%	70:30
5b	4-ClPh	*c*Hex	Ph_3Si	Ph	59%	70:30
5c	2-Thienyl	*c*Hex	Ph_3Si	Ph	21%	–
5d	Ph	*c*Hex	*t*BuPh$_2$Si	Ph	34%	70:30
5e	Ph	*c*Hex	Ac	Ph	72%	70:30
5f	Ph	*c*Hex	*t*BuAc	Ph	83%	70:30
5g	Ph	*n*Bu	Ph_3Si	Ph	56%	70:30
5h	Ph	*c*Hex	Ph_3Si	4-BrPh	69% (73%)[b)]	70:30
5i	3-MePh	*c*Hex	Ph_3Si	4-BrPh	74%	70:30
5j	Ph	*c*Hex	Ph_3Si	4-MePh	68%	70:30
5k	Ph	*c*Hex	Ph_3Si	4-MeOPh	35%	70:30

[a)] Isolated yield after column chromatography, referred to the sum of diastereoisomers.
[b)] Reaction conducted on 1 mmol scale.

benzils with electron-donating substituents are less reactive: indeed, compound **5k** was isolated in a reduced yield, while the reaction did not occur in the presence of 4-Me$_2$N-substituted benzil.

Next, we moved to study the adoption of different 1,2-dicarbonyl derivatives to evaluate possible site selectivities associated with the 2P-K-4CR. We therefore subjected mono 4-methoxy benzil **4b** to our optimized reaction conditions, which led to the formation of a mixture of regioisomers **5l-a** and **5l-b** in an overall 53% yield of isolated products (**Scheme 3**, top). We further explored the use of methyl benzoyl formate **4c** in the multicomponent process. After several attempts, the irradiation with two different wavelengths was found crucial for the positive outcome of the reaction. Thus, we preliminarily carried out the three-component K-3CR process at 450 nm, while it was necessary the adoption of 405 nm to photoexcite methyl benzoylformate and trigger the desired photocycloaddition. Pre-isolation of the olefin was not necessary; however, and compound **5m** could be isolated in moderate yield (24%) as a single regioisomer when adopting a sequential 450/405 nm irradiation (Scheme 3, middle).

Finally, we explored the possibility to further elaborate the oxetane ring, by removing the silyl protecting group. Deprotection of **5h** with HF/pyridine resulted in the isolation of ketoamide **6**, after cyclic hemiacetal ring opening (Scheme 3, bottom). In contrast, when tetrabutylammonium fluoride was used instead, a complex mixture was isolated, probably due to the peculiar reactivity of the ketoamide under these conditions, as previously reported by us.[24]

3. Computational Studies

To rationalize the mechanism of the reported 2 P-K-4CR, we undertook a computational investigation based on our precedent work describing the photocycloaddition between ketenes and benzils.[15] Thus, we adopted density functional theory at the (U)-B3LYP/6-311+G(d,p) level of theory as implemented in the Gaussian16 software. Geometries were fully optimized in the gas phase, while solvent effect (dichloromethane bulk) was included through single-point calculations at the same level of theory by employing an implicit model. In our previous work, we demonstrated that, during the formation of oxetanone **D** (see Scheme 2), a triplet 1,4-diradical is initially formed, while cyclization of the latter follows on the singlet surface upon intersystem crossing from the triplet to the more stable singlet manifold. The latter surface crossing may take place at the 1,4-diradical intermediate level or in the early stages of the cyclization step, where the two surfaces lie near to each other.[15] Since we do not expect significant mechanistic differences in the present 2P-K-4CR transformation, we decided to focus our attention on rationalizing the associated stereochemical output.

Starting from the collected X-Ray structures, we optimized the geometries of both diastereoisomers of product **5a**, namely $\mathbf{5a_M}$ and $\mathbf{5a_m}$, confirming that the major one is more stable than the minor by ≈4 kcal mol^{-1} at the considered level of theory (see Section S6.1, Supporting Information, for further details). However, to speed up calculations, we conveniently adopted simplified model structures, wherein bulky groups were substituted with smaller moieties, while aromatic phenyl groups were maintained where appropriate to avoid introducing any electronic bias with respect to experimental results. Thus, the actual reaction sequence considered for the present computational modelling is depicted in **Scheme 4**. As a first point, we verified that the same relative stability trend observed for the diastereoisomers of **5a** was maintained also in the case of the corresponding products, tagged as $\mathbf{P_M}$ and $\mathbf{P_m}$, related to the simplified process. Indeed, $\mathbf{P_M}$ is predicted to be more stable than

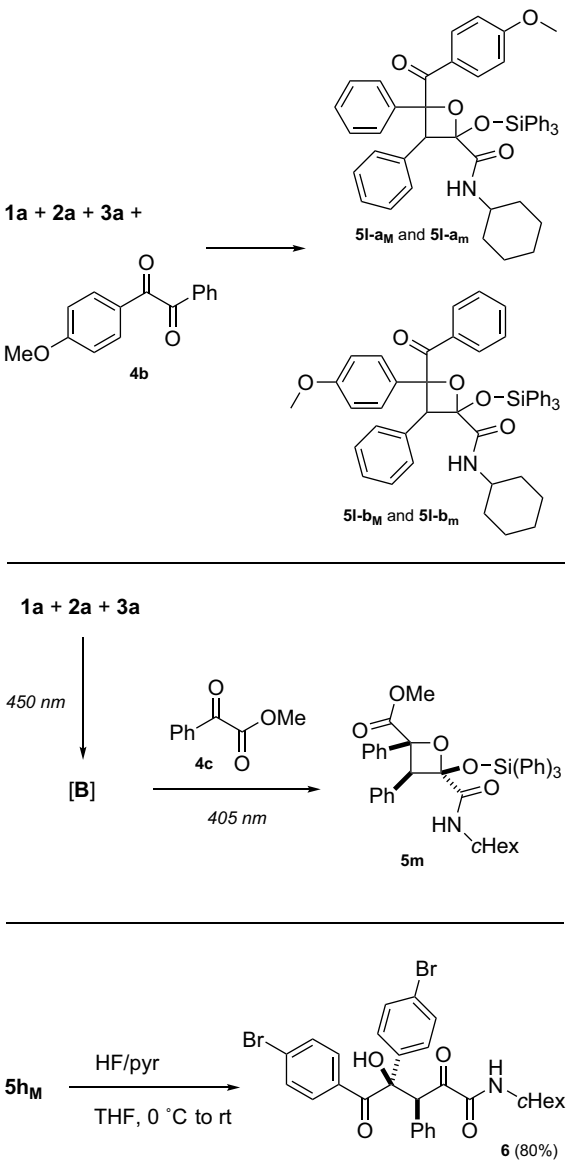

Scheme 3. 2-Photon ketene 4-component reaction with unsymmetrical benzil 7 (top) and methyl benzoylformate (middle); ring-opening of the oxetane ring mediated by HF/pyridine (bottom).

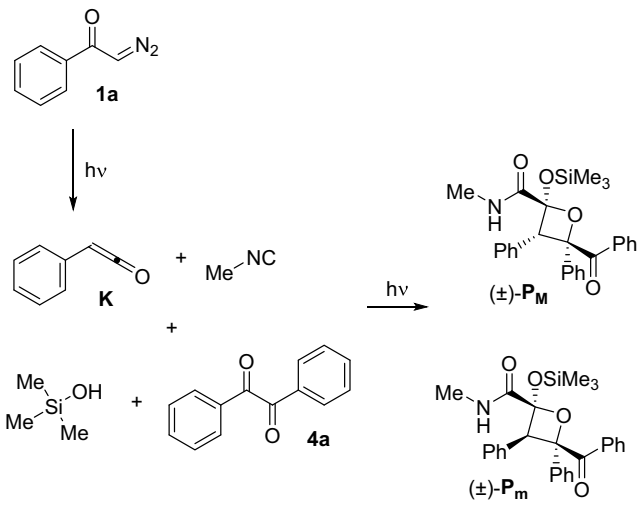

Scheme 4. Simplified model reaction considered in the computational study.

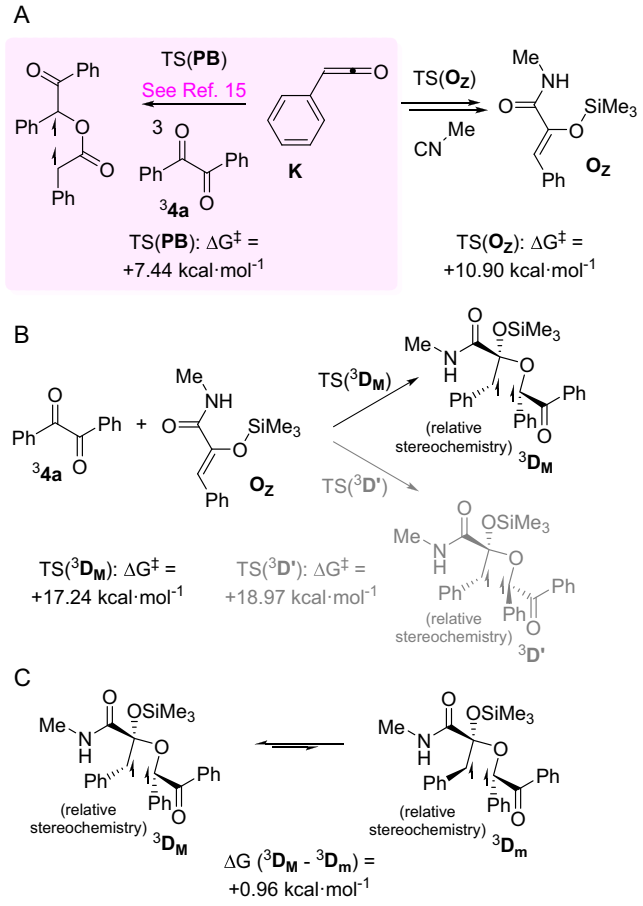

Scheme 5. Different reaction steps studied computationally: A) reactivity of the photogenerated ketene **K** with isocyanide to kick off the SK-3CR (right-hand side) or with excited benzil ^{3}**4a** to initiate previously reported photocycloaddition[15] (left-hand side); B) stereochemistry aspects in the reactivity of excited benzil ^{3}**4a** with **Oz**; and C) interconversion of triplet diradicals $^3\mathbf{D_M}$/$^3\mathbf{D_m}$.

$\mathbf{P_m}$ by 2.83 kcal mol^{-1} (see Section S6.1, Supporting Information, for further details).

First of all, we considered the formation of olefin $\mathbf{O_Z}$, characterized by an exclusive *Z* stereochemistry, through the previously reported SK-3CR reactivity.[19] As typical of multicomponent processes, such derivative is formed through an intricate, yet well-orchestrated sequence of steps. The full description of such pathway is beyond the scope of the present computational survey, therefore we limited our modelling to the initial step, namely the addition of the isocyanide to the photogenerated ketene **K** (**Scheme 5**a, right-hand side). Such step takes place through transition state TS($\mathbf{O_Z}$), which is characterized by an energy barrier ($\Delta G^{\ddagger}$) of +10.90 kcal mol^{-1}. This reactivity manifold is in direct competition with the

photocycloaddition between the ketene (**K**) and the (triplet)-excited state of benzil (^{3}**4a**; see Scheme 5a, left-hand side), a reactivity recently reported by us and described computationally at the same level of theory adopted here.[15] Thus, by comparing the activation energies of these two steps, namely TS(**PB**) (characterized by $\Delta G^{\ddagger} = +7.44$ kcal mol^{-1})[15] and TS($\mathbf{O_Z}$), it may be concluded that the photochemical pathway should be favored over the thermal one (in this case $\Delta\Delta G^{\ddagger} \approx 3.5$ kcal mol^{-1}). As a matter of fact, the photocycloaddition pathway, despite being characterized by a smaller activation energy, is disfavored over the SK-3CR, since the probability that the ketene **K** encounters the triplet excited state of benzil ^{3}**4a**, present in solution in a tiny concentration, is much lower than its possibility to combine with isocyanide, present in a much higher concentration.

We next moved on to study the photochemical process by modeling the reactivity between $\mathbf{O_Z}$ and ^{3}**4a** (Scheme 5b). Also based on our previous work,[15] such step involves the formation of a C—O bond and leads to the formation of a (triplet) diradical intermediate tagged ^{3}**D**. Furthermore, this step is expected to control the relative stereochemistry at C-2 and C-4 of the final oxetane ring. As reported in Scheme 5b, the approach between $\mathbf{O_Z}$ and ^{3}**4a** can occur through two different trajectories, characterized by transition states TS($^3\mathbf{D_M}$) and TS(^{3}**D'**) with a $\Delta\Delta G^{\ddagger}$ of ≈1.7 kcal mol^{-1} in favor of the former (see **Figure 3**a). Indeed, TS($^3\mathbf{D_M}$) leads to a triplet diradical intermediate showing the amide and the benzoyl groups in a *cis* arrangement (see structure $^3\mathbf{D_M}$), in agreement with the actual experimental output. We also note that both TS($^3\mathbf{D_M}$) and TS(^{3}**D'**) are characterized by a hydrogen bonding interaction between the N—H and the C=O group, which may be an important non-covalent interaction determining the observed regioselectivity for the C—O bond forming step (see Figure 3a and Section S6.2, Supporting Information).

Finally, we studied the geometry of the triplet diradical $^3\mathbf{D_M}$ (see Figure 3b) arising from TS($^3\mathbf{D_M}$), since its behavior has a direct impact on the stereochemistry of the final product, in particular for what concerns the (not yet established) configuration at C-3 of the oxetane ring (Scheme 5c). Accordingly, while the direct cyclization of $^3\mathbf{D_M}$ delivers $\mathbf{P_M}$, rotation along the C_2—C_3 bond leads to the formation of triplet diradical intermediate $^3\mathbf{D_m}$, from which $\mathbf{P_m}$ can be obtained. Thus, $^3\mathbf{D_m}$ lies a mere 0.96 kcal·mol^{-1} above $^3\mathbf{D_M}$ and can be easily populated through a facile process, characterized by a modest energy barrier (<3.5 kcal mol^{-1}; see Section S6.3, Supporting Information).

Overall, the present computational analysis allows to rationalize the stereochemistry of the obtained products, in particular for what concern the relative stereochemistry at C-2/C-4 of the oxetane ring also clarifying the reasons for the observed variability at C-3. As for the latter aspect, two minima with slightly different energy content have been located for the involved triplet diradical intermediate. Thus, according to the simulations, they may easily interconvert between each other prior to the cyclization event, coherently with the experimental observations.

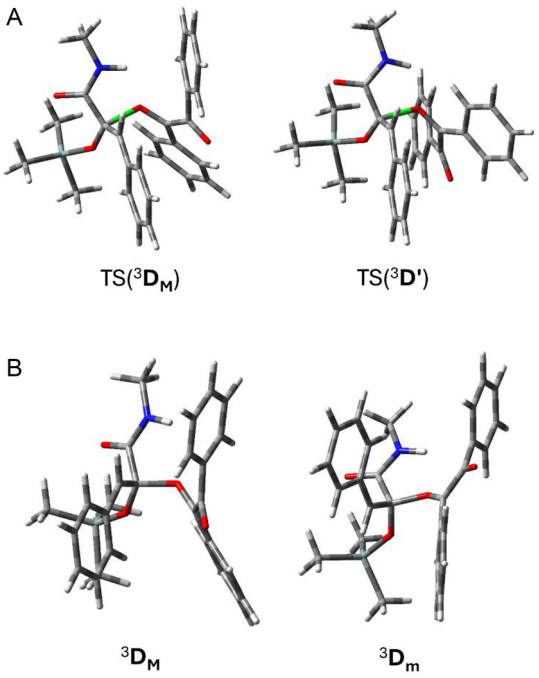

Figure 3. Selected geometries optimized in the present computational analysis. A) geometries of transition states (TS); B) geometries of triplet diradicals (D).

4. Conclusions

In conclusion, we have reported a novel doubly activated photochemical multicomponent reaction (PMCR) for the synthesis of highly functionalized oxetanes. The present 2-photon 4-component reaction, tagged 2P-K-4CR, involves the simultaneous activation of diazoketones and benzils with visible light, resulting in the formation of ketenes and the population of triplet excited benzils, respectively. However, these species do not engage in the previously reported Paterno–Büchi-type [2 + 2] cycloaddition;[15] instead, under the present reaction conditions comprising isocyanides and silanols (or carboxylic acids) as well, they prefer to follow a different path. Thus, they afford complex heterocycles with the simultaneous formation of four new bonds and three stereogenic centers, including two quaternary ones. Remarkably, the reaction is completely regioselective and highly stereoselective, with the formation of only two diastereoisomers. Characterization techniques, including NMR and X-Ray analysis, and a computational analysis supported the rationalization of all aspects related to the process, elucidating also details on the reaction mechanism and

products stability. Furthermore, an optimization of the reaction conditions was carried out using DoE, enabling the synthesis of a variety of oxetane compounds with good versatility.

5. Experimental Section

Experimental details and analytical data for all new compounds are available in Supporting Information. The authors have cited additional references within Supporting Information.[25–31]

Acknowledgements

The authors acknowledge the CINECA award under the ISCRA initiative, for the availability of high-performance computing resources and support. D.R. acknowledges support from the Ministero dell'Università e della Ricerca (MUR) and the University of Pavia through the program "Dipartimenti di Eccellenza 2023–2027".

Open access publishing facilitated by Universita degli Studi di Genova, as part of the Wiley - CRUI-CARE agreement.

Conflict of Interest

The authors declare no conflict of interest.

Data Availability Statement

Research data are not shared.

References

[1] J. A. Bull, R. A. Croft, O. A. Davis, R. Doran, K. F. Morgan, *Chem. Rev.* **2016**, *116*, 12150.
[2] J. Li, B. Yuan, C. Li, Z. Zhao, J. Guo, P. Zhang, G. Qu, Z. Sun. *Angew. Chem. Int. Ed.* **2024**, *63*, e202411326.
[3] C. Li, X. Yin, S. Wang, S. Sui, J. Liu, X. Sun, J. Di, R. Chen, D. Chen, Y. Han. *Angew. Chem. Int. Ed.* **2024**, *63*, e202407070.
[4] T. Sone, G. Lu, S. Matsunaga, M. Shibasaki. *Angew. Chem.* **2009**, *121*, 1705 and references therein.
[5] E. D. Butova, A. V. Barabash, A. A. Petrova, C. M. Kleiner, P. R. Schreiner, A. A. Fokin. *J. Org. Chem.* **2010**, *75*, 6229 and references therein.
[6] D. Qi, J. Bai, H. Zhang, B. Li, Z. Song, N. Ma, L. Guo, L. Song, W. Xia. *Green Chem.* **2022**, *24*, 5046 and references therein.
[7] M. R. Gatazka, S. G. Parikh, K. A. Rykaczewski, C. S. Schindler. *Synthesis* **2024**, *56*, 2513 and references therein.
[8] M. D'Auria. *Photochem. Photobiol. Sci.* **2019**, *18*, 2297.
[9] K. A. Rykaczewski, C. S. Schindler. *Org. Lett.* **2020**, *22*, 6516.
[10] R. Tinelli, D. Ravelli, A. Basso, S. C. Tarantino, L. Capaldo. *Photochem. Photobiol. Sci.* **2022**, *21*, 695.
[11] J. Mateos, A. Vega-Peñaloza, P. Franceschi, F. Rigodanza, P. Andreetta, X. Companyó, G. Pelosi, M. Bonchio, L. Dell'Amico. *Chem. Sci.* **2020**, *11*, 6532.
[12] P. Franceschi, S. Cuadros, G. Goti, L. Dell'Amico. *Angew. Chem. Int. Ed.* **2023**, *62*, e202217210.
[13] S. Garbarino, D. Ravelli, S. Protti, A. Basso, *Angew. Chem. Int. Ed.* **2016**, *55*, 15476.
[14] G. A. Coppola, S. Pillitteri, E. V. Van der Eycken, S.-L. You, U. K. Sharma, *Chem. Soc. Rev.* **2022**, *51*, 2313.
[15] F. Minuto, E. Farinini, S. De Negri, R. Leardi, D. Ravelli, P. Solokha, A. Basso, *J. Flow Chem.* **2024**, *14*, 149.
[16] A. Basso, L. Banfi, S. Garbarino, R. Riva, *Angew. Chem. Int. Ed.* **2013**, *52*, 2096.
[17] S. Garbarino, L. Banfi, R. Riva, A. Basso, *J. Org. Chem.* **2014**, *79*, 3615.
[18] F. Ibba, P. Capurro, S. Garbarino, M. Anselmo, L. Moni, A. Basso, *Org. Lett.* **2018**, *20*, 1098.
[19] P. Capurro, C. Lambruschini, P. Lova, L. Moni, A. Basso, *J. Org. Chem.* **2021**, *86*, 5845.
[20] Deposition numbers 2402672 (for $5a_M$) and 2402789 (for $5a_m$) contain the supplementary crystallographic data for this paper. These data are provided free of charge by the joint Cambridge Crystallographic Data Centre and Fachinformationszentrum Karlsruhe Access Structures service.
[21] J. Workman Jr., *Chemometr. Intell. Lab. Syst.* **2002**, *60*, 13.
[22] R. Leardi. *Anal. Chim. Acta* **2009**, *652*, 161.
[23] B. Benedetti, V. Caponigro, F. Ardini. *Crit. Rev. Anal. Chem.* **2022**, *52*, 1015.
[24] E. Bergamaschi, P. Capurro, C. Lambruschini, R. Riva, A. Basso. *Eur. J. Org. Chem.* **2019**, 5992.
[25] R. Leardi, in *Encyclopedia of Analytical Chemistry*, John Wiley & Sons, Ltd, Chichester, UK, **2018**, pp. 1-11.
[26] L. Eriksson, E. Johansson, N. Kettaneh-Wold, C. Wikström, S. Wold, *Design of Experiments- Principles and Applications*, Umetrics Academy, Umea (S) **2000**.
[27] R. Leardi, C. Melzi, G. Polotti. CAT (Chemometric Agile Tool), http://gruppochemiometria.it/index.php/software. (access: May 2025).
[28] M. J. Frisch, G. W. Trucks, H. B. Schlegel, G. E. Scuseria, M. A. Robb, J. R. Cheeseman, G. Scalmani, V. Barone, G. A. Petersson, H. Nakatsuji, X. Li, M. Caricato, A. V. Marenich, J. Bloino, B. G. Janesko, R. Gomperts, B. Mennucci, H. P. Hratchian, J. V. Ortiz, A. F. Izmaylov, J. L. Sonnenberg, D. Williams-Young, F. Ding, F. Lipparini, F. Egidi, J. Goings, B. Peng, A. Petrone, T. Henderson, D. Ranasinghe, et al., Gaussian 16, Revision C.01, Gaussian, Inc., Wallingford CT **2019**.
[29] F. Minuto, C. Lambruschini, A. Basso.*Eur. J. Org. Chem.* **2021**, 3270.
[30] J. Zhang, W. Chen, H. Dayun, X. Zeng, X. Wang, Y. Hu. *J. Org. Chem.* **2017**, *82*, 9171.
[31] G. N. Rao, G. Sekar. *New J. Chem.* **2023**, *47*, 3167.